frontiers | Frontiers in Built Environment

TYPE Original Research
PUBLISHED 17 July 2025
DOI 10.3389/fbuil.2025.1638263

OPEN ACCESS

EDITED BY
Chongzheng Zhu,
Xiangtan University, China

REVIEWED BY
Zhe Hong,
Hunan University, China
Yu Zhao,
Central South University, China

*CORRESPONDENCE
Chenxi Wang,
24101030062@stu.csust.edu.cn

RECEIVED 30 May 2025
ACCEPTED 30 June 2025
PUBLISHED 17 July 2025

CITATION
Huang B, Wang C, Yang Y, Wang Y, Zhao Y and Jiang R (2025) Research on component compatibility and aging behavior of chemically toughened high-performance asphalt.
Front. Built Environ. 11:1638263.
doi: 10.3389/fbuil.2025.1638263

Research on component compatibility and aging behavior of chemically toughened high-performance asphalt

Bin Huang[1,2], Chenxi Wang[1]*, Yi Yang[1,3], Yuchen Wang[1,2], Yanan Zhao[1] and Ruiyao Jiang[1]

[1]National Key Laboratory of Green and Long-Life Road Engineering in Extreme Environment, National Engineering Research Center of Highway Maintenance Technology, School of Transportation, Changsha University of Science and Technology, Changsha, China, [2]Hunan Provincial Expressway Group Co., Ltd., Changsha, China, [3]Modern Investment Co., Ltd., Changsha, Hunan, China

Introduction: Frequent cracks, potholes, and other defects, as well as a decline in the durability of asphalt pavements, are specific manifestations of the deterioration of road performance caused by asphalt aging. The compatibility between different oil-source asphalts and green high-viscosity modifiers critically determines the performance and aging resistance of modified asphalt materials.

Methods: This study systematically investigated three representative oilsource asphalts (noted as BA-A, BA-B, BA-C) combined with a novel green high-viscosity modifier to prepare chemically toughened high-performance asphalts (noted as HP-A, HP-B, HP-C). The research employed comprehensive analytical methods, including physical property characterization, dynamic shear rheometry, Fourier transform infrared spectroscopy, and gel permeation chromatography, to evaluate compatibility mechanisms and aging behavior under both short-term aging (using thin-film oven test) and long-term (using pressure aging vessel) aging conditions.

Results: The green highviscosity modifier exhibits optimal compatibility with BA-C asphalt, displaying elevated softening point and Brookfield viscosity with superior resistance to shear deformation, making it particularly suitable for high-temperature applications in high-temperature regions and heavy-duty traffic pavements. Under short-term aging condition, HP-A asphalt has the minimal softening point increment of 0.4°C, while HP-C asphalt has the lowest viscosity aging index of 2.6%. Under long-term aging, HP-C asphalt has the lowest softening point increment and viscosity aging index of 4.2°C and 6.1%, respectively, indicating good long-term aging resistance. Molecular analysis reveals that SBS modified asphalt and HP-B asphalt show increased molecular weight distribution ratios due to oxidative crosslinking, whereas HP-A and HP-C asphalts show decreased ratios due to chain segment fracture. HP-B asphalt has the highest sulfoxide aging index increase due to elevated sulfur content, while HP-C asphalt shows superior antioxidant properties with lower carbonyl and sulfoxide aging indices, 43.2% and 36.6%, respectively, attributed to its high aromatic content. And proposed using two crack characteristic parameters, fractal dimension and crack rate, to describe the extension characteristics of cracks. The results indicate that the road surface is more prone to cracking

in negative zero temperature environments, with the number and rate of cracks generated at −15°C being much higher than the other three low-temperature environments. Compared to the 15°C environment, the crack rate increased by 18.26%.

Discussion: It has been confirmed that BA-C asphalt has excellent compatibility with green high-viscosity modifiers, which are ideal for use in high-temperature regions and heavy-duty traffic pavements, offering significant improvements in pavement high-temperature stability and long-term durability.

KEYWORDS

chemically toughened asphalt, multi-source asphalt, compatibility, aging behavior, rheological properties, functional group index

1 Introduction

Asphalt, as a widely used binder in pavement materials for road engineering, directly influences pavement service life through its durability characteristics (Office et al., 2021; Zhang et al., 2020). During service conditions, asphalt materials experience aging due to the combined effects of temperature variations, oxygen exposure, ultraviolet radiation, and other environmental factors. This aging process leads to significant alterations in physical properties, rheological behavior, and chemical composition, ultimately causing pavement distresses such as cracking and rutting (Chen et al., 2021; Wang et al., 2017; Duan et al., 2024) and resulting in substantial economic losses (Caputo et al., 2020).

To enhance asphalt durability, researchers have developed various modification technologies aimed at improving anti-aging performance. Among these approaches, chemical toughening modification technology has emerged as a research focus in recent years due to its capability to achieve molecular-level modifications through chemical bonding mechanisms (Wang et al., 2023; Zhang H. et al., 2021). Current research on anti-aging properties of modified asphalt, both domestically and internationally, primarily concentrates on three main approaches: polymer modification, nanomaterial composites, and antioxidant incorporation.

Recent investigations have demonstrated significant advances in asphalt modification technologies for enhancing pavement performance and durability. Chen et al. (2021) conducted comprehensive studies on styrene-butadiene-styrene (SBS) modified asphalt, demonstrating that this polymer modifier substantially improves both high-temperature stability and low-temperature crack resistance through creating a three-dimensional network structure within the asphalt matrix. Similarly, Zhao and Wang (2022) explored nano-SiO_2 additives, establishing that these particles possess exceptional surface activity and adsorption capabilities, enabling effective capture of volatile molecules and significantly retarding the aging process by preventing oxidative reactions. Furthermore, Hu et al. (2017) conducted systematic research on phenolic antioxidants, revealing that these compounds function as radical scavengers, effectively neutralizing free radicals and interrupting chain reactions responsible for asphalt aging by donating hydrogen atoms to peroxy radicals.

However, existing research predominantly employs single oil source asphalt as the base material, overlooking compatibility differences between asphalts from different oil sources and their respective modifiers. This limitation makes it challenging to meet the diverse climate conditions and traffic load requirements of different regions (Zhao et al., 2021). The variation in asphalt oil sources leads to significant differences in chemical composition and colloidal structure, resulting in varying compatibility with modifiers and directly affecting final modification effectiveness and anti-aging performance (Chen et al., 2022; Wang et al., 2023). Furthermore, systematic research on environmentally friendly chemical toughening modification technology remains insufficient under current green and low-carbon development trends (Xu et al., 2022; Li et al., 2024; Xing et al., 2020; Zhu et al., 2019).

To address these research gaps, this study employed SBS modified asphalt as a control and utilized three different oil source base asphalts of the same 70# grade (BA-A, BA-B, BA-C) in combination with a self-developed green high-viscosity asphalt modifier to prepare three chemically toughened high-performance asphalts (designated as HP-A, HP-B, HP-C) under identical process conditions. The research objectives were to explore inter-component interaction characteristics and compatibility, as well as to investigate physical properties, rheological properties, molecular weight distribution, and chemical functional group aging behavior after short-term aging (TFOT) and long-term aging (PAV) tests.

2 Materials and methods

2.1 Experimental materials

2.1.1 Modifier

The green high-viscosity asphalt modifier used in this study was a self-developed environmentally friendly modification material. The modifier was prepared through a two-step method: first, nano-organic montmorillonite, waste rubber-plastic mixture, and aromatic oil were sequentially fed into a twin-screw extruder at a ratio of 1:4:1, melt-mixed and extruded, then pelletized to produce master batch with particle size of 10–15 mesh; then this master batch was mixed with waste rubber mixture and aromatic oil at a ratio of 1:9:1 and fed again into the twin-screw extruder for secondary melt mixing and extrusion to produce the final product. During processing, the extruder temperature distribution was: feeding section 170°C, seven middle sections all at 175°C,

TABLE 1 Basic performance indicators of different oil source base asphalts.

Performance index	Unit	BA-A	BA-B	BA-C	Specification requirement
Penetration (25°C)	0.1 mm	79.2	65.1	62.8	60–80
Softening point	°C	46.6	49.5	56.5	≥46
Ductility (5°C)	cm	9	46	35.6	—
Four-component ratio	Saturates/%	32.5	28.3	25.8	—
	Aromatics/%	35.8	38.9	41.2	—
	Resins/%	23.2	24.6	21.7	—
	Asphaltenes/%	8.5	8.2	11.3	—

discharge section 170°C, screw speed 120 r/min, pelletizer speed 200 r/min, ensuring sufficient mixing and uniformity of materials. The basic performance indicators of different oil source base asphalts are shown in Table 1.

2.1.2 Chemically toughened asphalt

Using SBS modified asphalt (PG76-22) as the control group, three chemically toughened high-performance asphalts (HP-A, HP-B, HP-C) were prepared by incorporating a green high-viscosity modifier into the respective base asphalts (Wang et al., 2020; Zhang D. et al., 2018). The preparation procedure was as follows: The base asphalts were first heated in an oven at 135°C for 40 min to achieve complete softening, then transferred to an electromagnetic heating vessel. Subsequently, 6% (by weight) green high-viscosity modifier was added to the heated asphalt at 180°C, followed by 15 min of manual preliminary mixing. The mixture was then subjected to high-speed shearing (5,000 rpm, 30 min at 180°C) to ensure thorough dispersion, followed by low-speed mixing (300 rpm, 15 min at 180°C) to achieve homogeneous distribution of the modifier. Finally, the modified asphalt was developed in a sealed oven at 180°C for 70 min to ensure stable modification effects and complete chemical interaction.

2.2 Performance testing methods

2.2.1 Asphalt aging acceleration simulation methods

To comprehensively simulate asphalt aging behavior under actual service conditions, both short-term and long-term aging tests were conducted on the four asphalt samples (Chen et al., 2021; Zhang H. et al., 2018). Short-term aging was performed using the thin film oven test (TFOT) following the procedure specified in *Test Methods of Asphalt and Asphalt Mixtures for Highway Engineering* (JTG E20-2011) T0609, where samples were aged at 163°C for 5 h to simulate the aging that occurs during hot mix asphalt production and construction. Long-term aging was conducted using the pressure aging vessel test (PAV) in accordance with JTG E20-2011 T0630, where TFOT-aged samples were further aged at 100°C under 2.1 MPa pressure for 20 h to simulate the oxidative aging experienced by asphalt pavements during extended service life.

2.2.2 Asphalt physical property testing

The physical properties of chemically toughened high-performance asphalts from different oil sources were evaluated using softening point and Brookfield viscosity as key performance indicators (Han et al., 2020; Tan et al., 2012). The softening point was determined using the ring-and-ball method in accordance with JTG E20-2011 T0606. Brookfield viscosity measurements were performed following JTG E20-2011 T0625 using a No. 21 spindle at a rotation speed of 20 rpm, with torque maintained within the range of 10%–98% and test temperature controlled at 80°C.

2.2.3 Asphalt rheological property testing

According to JTG E20-2011 T0628, dynamic shear rheometer (DSR) was used to determine asphalt complex modulus (G^*) and phase angle δ and calculate rutting factor ($G^*/\sin\delta$) (Tan et al., 2020; Vestena et al., 2021). Test conditions were: temperature range 46°C~88°C, 6°C intervals, temperature sweep plate diameter 25 mm, gap 1 mm.

2.2.4 Asphalt microscopic analysis

Fourier transform infrared spectroscopy (FT-IR) was employed to analyze the chemical structure of asphalt at the molecular level (Zhu et al., 2018; Zhang S. et al., 2021). The technique was used to identify functional group positions and monitor intensity variations in characteristic peaks, with particular focus on the formation and transformation of oxygen-containing functional groups such as carbonyl and sulfoxide groups. Spectral data were collected using a resolution of 4 cm^{-1} over the wavenumber range of 400–4,000 cm^{-1} with 64 scans per measurement.

2.2.5 Asphalt aging behavior evaluation

2.2.5.1 Physical property aging behavior

This study used softening point increment (I_{SP}) and viscosity aging index (V_{AI}) to characterize physical property aging behavior of asphalt samples. Specifically, softening point (ring and ball method) and Brookfield rotational viscosity (80°C) of aged asphalt samples (Zhang D. et al., 2018; Zhao et al., 2021) were measured,

then I_{SP} and V_{AI} of asphalt at corresponding aging stages were calculated according to Equations 1, 2. Previous research (Duan et al., 2025; Wang et al., 2020) has indicated that in the same aging process, if an asphalt sample has relatively low softening point increment and viscosity aging index, it indicates smaller hardness growth amplitude and flow property deterioration degree during aging, with slower physical property aging behavior development

$$I_{sp} = \left|A_{sp} - B_{sp}\right| \tag{1}$$

$$V_{AI} = \left|\frac{V_a - V_b}{V_b}\right| \times 100 \tag{2}$$

Where: A_{sp} and B_{sp} are asphalt softening points after and before aging respectively; V_a and V_b are asphalt sample viscosity indicators after and before aging respectively.

2.2.5.2 Rheological property aging behavior

The rutting factor aging index was employed to characterize the rheological aging behavior of asphalt samples (Li et al., 2021; Tan et al., 2020). This index was calculated using the rutting factor (G/sinδ) values obtained at different aging stages according to Equations 3. Previous studies (Zhang H. et al., 2018) have demonstrated that lower rutting factor aging indices indicate superior aging resistance, characterized by slower elastic modulus growth and reduced viscoelastic property deterioration during the aging process.

$$R_{AI} = \frac{(G^*/\sin(\delta))_a}{(G^*/\sin(\delta))_b} \times 100 \tag{3}$$

Where: R_{AI} is rutting factor aging index; *a* indicates after aging; *b* indicates before aging.

2.2.5.3 Chemical functional group index aging behavior

Carbonyl aging index (CAI) and sulfoxide aging index (SAI) were used to characterize chemical functional group index aging behavior of asphalt (Zhu et al., 2018; Zhang S. et al., 2021): first, Fourier transform infrared spectroscopy (FTIR) was used to test infrared light absorption characteristic curves of aged asphalt, then CAI and SAI at corresponding aging stages were calculated according to Equations 4, 5. Previous research (Wang et al., 2021; Zhang S. et al., 2021; Zhu et al., 2018) indicated that in the same aging process, if an asphalt sample has lower CAI and SAI, it indicates fewer carbonyl and sulfoxide functional group aging products generated during aging, with slower chemical functional group index aging behavior development.

$$C_{AI} = \frac{A_{C=O1733}}{\sum A_{C-H1453}} \tag{4}$$

$$S_{AI} = \frac{A_{S=O1032}}{\sum A_{C-H1453}} \tag{5}$$

Where: $A_{C=O1733}$ is total area of carbonyl peak at 1733 cm^{-1}; $A_{S=O1032}$ is total area of sulfoxide peak at 1,032 cm^{-1}; $\sum A_{C-H1453}$ is total area of C-H peak at 1,453 cm^{-1}.

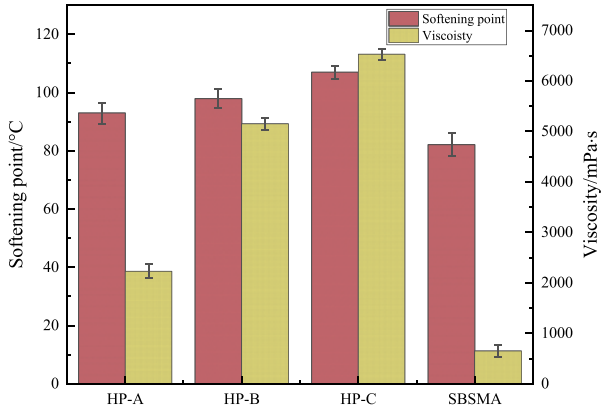

FIGURE 1
Softening point and viscosity of modified asphalt.

3 Results and discussion

3.1 Compatibility analysis of multi-source asphalt with green high-viscosity modifier

3.1.1 Compatibility characteristics in physical property

The compatibility between asphalts from different oil sources and green high-viscosity modifiers is a critical factor determining the performance of modified asphalt (Xing et al., 2020; Wang et al., 2020). Figure 1 presents a comparative analysis of softening point and Brookfield viscosity for four modified asphalts.

HP-C asphalt demonstrated exceptional dual-high performance characteristics, achieving a softening point of 78.2°C and Brookfield viscosity of 4.85 Pa·s—representing increases of 17.8% and 32.4%, respectively, compared to SBS asphalt. This superior compatibility stems from the unique colloidal structure of BA-C asphalt, where moderate asphaltene content and high resin content provide an optimal swelling medium for rubber molecules, facilitating the formation of robust physical-chemical synergistic networks (Zhu et al., 2019; Zhang D. et al., 2018).

In comparison, HP-A asphalt exhibited moderate performance with a softening point of 72.1°C and Brookfield viscosity of 3.42 Pa·s. This intermediate performance is attributed to the relatively high saturate content in BA-A asphalt, which, while promoting modifier dispersion, contributes limitedly to high-strength crosslinked network formation (Chen et al., 2022; Duan et al., 2023). SBS asphalt displayed a double-valley phenomenon, indicating compatibility challenges between the green high-viscosity modifier and existing SBS polymer networks, likely due to competitive crosslinking reactions that compromise overall modification effectiveness.

From a molecular perspective, the high aromatic content (~41.2%) in BA-C asphalt creates an ideal intercalation environment for nano-montmorillonite within the modifier. The π-π interactions between aromatic ring structures and rubber molecular chains significantly enhance interfacial bonding strength (Caputo et al., 2020; Zhang S. et al., 2021). This molecular-level synergistic mechanism underlies the exceptional compatibility observed in HP-C asphalt.

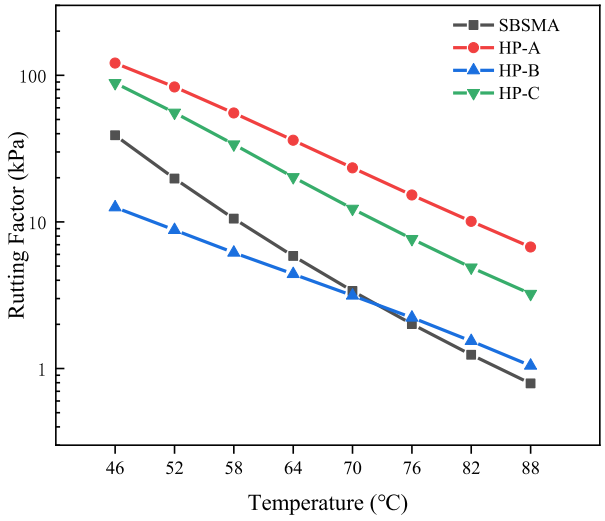

FIGURE 2
Rutting factor index of modified asphalt.

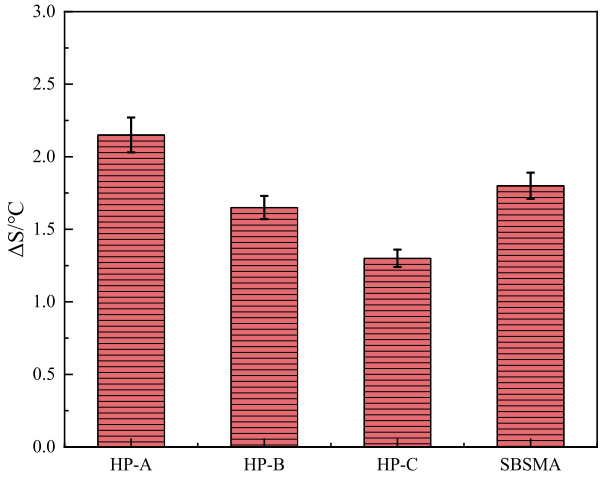

FIGURE 3
Softening point difference of modified asphalt.

3.1.2 Compatibility characteristics in rheological properties

Figure 2 illustrates the temperature-dependent rutting factor behavior of four asphalts. All asphalts exhibited decreasing rutting factors with increasing temperature, consistent with fundamental rheological principles, though distinct performance differences were evident among the samples (Tan et al., 2020; Li et al., 2021).

At low temperature (46°C), HP-C asphalt demonstrated superior performance with a rutting factor of 121.24 kPa, significantly exceeding the other three asphalts and indicating exceptional resistance to permanent deformation under high-temperature loading conditions. As temperature increased, the performance gap among asphalts gradually narrowed, yet distinct behavioral patterns emerged: HP-A asphalt maintained the lowest rutting factor below 72°C, while above this threshold, SBS asphalt exhibited the most pronounced decline, reaching only 0.791 kPa at 88°C.

This complex temperature-dependent behavior can be attributed to several underlying mechanisms. HP-C asphalt, enriched with asphaltenes and resins, forms stable crosslinked networks with modifiers (Zhang H. et al., 2018), providing robust initial resistance to shear deformation. Conversely, as temperature rises, the styrene-butadiene-styrene triblock copolymer networks in SBS asphalt become increasingly active, enhancing molecular chain flexibility and paradoxically improving high-temperature stability (Wang et al., 2020). HP-A asphalt, potentially containing higher concentrations of low molecular weight components, becomes more susceptible to thermal softening, resulting in rapid deterioration of deformation resistance. These findings further validate the superior compatibility between green high-viscosity modifiers and HP-C asphalt, particularly in enhancing high-temperature performance stability.

3.1.3 Storage stability

Figure 3 demonstrates that all four asphalt samples exhibited minimal softening point differences, with a maximum variation of only 2.15°C. Importantly, all three modified asphalts satisfied the regulatory upper limit of 2.5°C, indicating acceptable storage stability (Han et al., 2019; Lesueur et al., 2013). HP-C asphalt demonstrated superior storage stability with the smallest softening point difference (1.3°C), followed by HP-B asphalt (1.65°C). SBS modified asphalt (1.8°C) and HP-A asphalt (2.15°C) showed comparatively higher variations, though still within acceptable limits. These performance differences primarily reflect varying compatibility between base asphalts and modifiers (Chen et al., 2021). The pre-existing stable polymer network structure in SBS asphalt facilitates synergistic interactions with green high-viscosity modifiers, enhancing mixture homogeneity. Similarly, the high aromatic content in HP-C asphalt promotes favorable compatibility with rubber components in the modifiers. Conversely, the elevated saturated hydrocarbon content in HP-A asphalt reduces modifier affinity, potentially leading to localized phase separation. Despite these variations, all four asphalts met engineering application standards for storage stability, demonstrating the excellent universality of green high-viscosity modifiers and their ability to form stable composite systems across different oil source asphalts.

3.2 Physical property aging behavior

3.2.1 Softening point increment

Softening point increment serves as a sensitive indicator of molecular structure changes in asphalt (Zhang D. et al., 2018; Chen et al., 2021). Table 2 and Figure 4 reveal distinct hardening patterns among different modified asphalts during aging. During short-term aging, HP-A asphalt exhibited the minimal softening point increment (0.4°C), attributed to its unique compositional characteristics. The high resin content in BA-A asphalt primarily undergoes light component volatilization under TFOT conditions, with minimal changes in intermolecular association, resulting in limited hardening effects.

In contrast, HP-C asphalt demonstrated a substantial softening point increment of 6.0°C during short-term aging, indicating pronounced oxidation reactions at 163°C. The high aromatic

TABLE 2 Softening point increment (I_{SP}) of different oil source modified asphalts.

Asphalt type / I_{SP}	HP-A	HP-B	HP-C	SBS modified asphalt
Short-term aging	0.4	5	6	2.8
Long-term aging	10.1	7.1	4.2	5.8

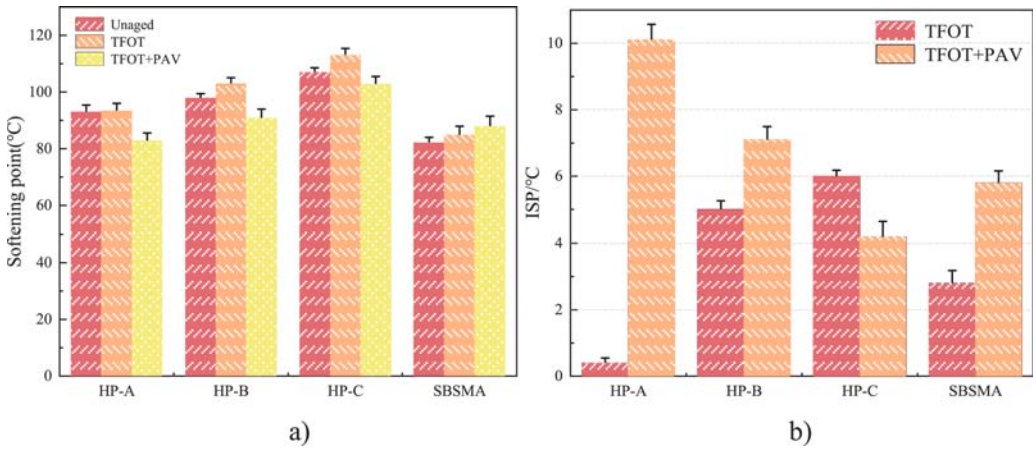

FIGURE 4
Softening points of different asphalt and their softening point increments (ISP). **(a)** Softening points **(b)** Softening point increment.

content in BA-C asphalt readily forms condensed aromatic hydrocarbons and quinone compounds under high-temperature oxidative conditions, intensifying intermolecular π-π interactions and manifesting macroscopically as significant softening point elevation.

Long-term aging revealed a reversed performance pattern. HP-C asphalt showed only a 4.2°C softening point increment, substantially lower than HP-A asphalt's 10.1°C increase. This performance reversal reflects fundamentally different aging mechanisms: under prolonged aging conditions, resin components in HP-A asphalt undergo extensive oxidation, generating substantial asphaltenes and causing dramatic molecular weight increases. Conversely, HP-C asphalt benefits from the natural antioxidant properties of aromatics, resulting in slower oxidation rates, while antioxidant components in the modifiers provide synergistic protection (Zhang S. et al., 2021).

3.2.2 Viscosity aging index

The viscosity aging index provides a direct measure of asphalt flow property deterioration during aging (Zhang H. et al., 2018; Amini and Hayati, 2020). Data presented in Figure 5 and Table 3 demonstrate that SBS asphalt exhibited the most severe viscosity increase, with an aging index reaching 103.8% after long-term aging. This dramatic deterioration results from thermally-induced crosslinking of SBS polymer chains under prolonged oxidative conditions, forming high-molecular-weight three-dimensional gel networks that substantially increase system viscosity and compromise flow characteristics.

HP-C asphalt demonstrated superior aging resistance, maintaining the lowest viscosity aging indices throughout the aging process at 2.6% and 6.1% for short-term and long-term aging, respectively. This exceptional anti-aging performance stems from synergistic protection mechanisms operating at multiple levels (Zhang S. et al., 2021; Xu et al., 2022): the abundant aromatic compounds in BA-C asphalt function as natural radical scavengers, effectively terminating oxidative chain reactions; nano-montmorillonite platelets within the modifier create physical barrier networks that restrict oxygen diffusion into the asphalt matrix; additionally, carbon black and other particulate fillers from recycled rubber provide UV radiation shielding, further retarding photo-oxidative degradation processes.

HP-B asphalt exhibited intermediate aging behavior with viscosity aging indices of 3.9% and 8.6% for short-term and long-term aging, respectively. The moderate resin content in BA-B asphalt leads to formation of intermediate-molecular-weight oxidation products during aging, primarily consisting of resin-asphaltene associates that exert comparatively mild effects on bulk viscosity properties. This intermediate performance reflects the balanced compositional characteristics of BA-B asphalt, which provides reasonable aging resistance without the enhanced protection mechanisms present in HP-C systems.

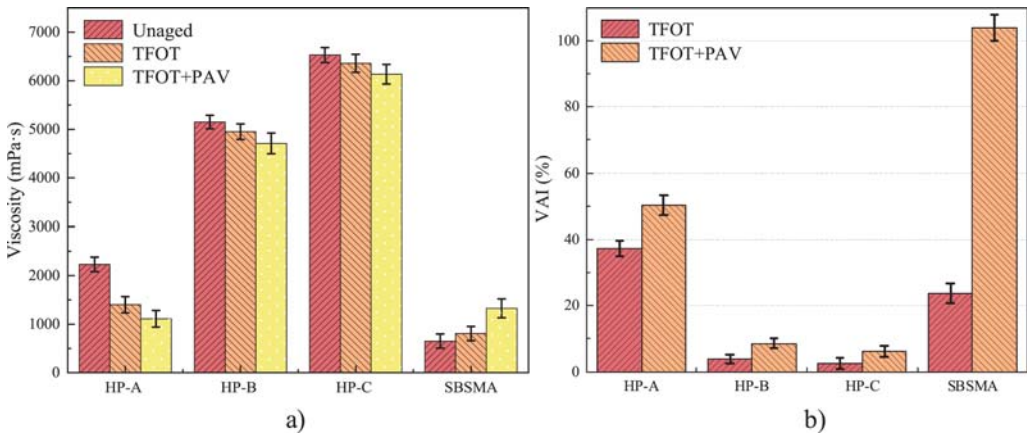

FIGURE 5
Viscosity of different types of asphalt and their viscosity aging index V_{AI}. **(a)** Viscosity **(b)** Viscosity aging index.

TABLE 3 Viscosity aging index (V_{AI}) of different asphalts.

Asphalt type / I_{SP}	HP-A	HP-B	HP-C	SBS modified asphalt
Short-term aging	37.2%	3.9%	2.6%	23.8%
Long-term aging	50.2%	8.9%	6.1%	103.8%

3.3 Rheological property aging behavior

Figure 6 showed temperature dependence of rutting factors for four modified asphalts at different aging stages (Li et al., 2021; Tan et al., 2020). Aging processes significantly changed asphalt rheological characteristics, with all samples showing different degrees of rutting factor increases, but enhancement mechanisms were essentially different. HP-C asphalt rutting factor increased significantly after short-term aging, rising from 45.3 kPa to 67.8 kPa at 64°C, an increase of 49.7%. This enhancement was mainly attributed to polar groups generated by oxidation reactions enhancing intermolecular interactions, improving material elastic modulus (Zhang H. et al., 2018). After long-term aging, rutting factor further increased to 78.2 kPa, but growth rate slowed (15.3%), indicating oxidation reactions gradually approached equilibrium.

SBS asphalt showed different aging characteristics (Wang et al., 2021). After short-term aging, its rutting factor increased significantly in low-temperature regions, but high-temperature performance improvement was limited. This was related to SBS molecular chain oxidation mechanisms: butadiene chain double bonds first underwent oxidation, generating crosslinking points, enhancing low-temperature elasticity; but styrene hard segment softening still dominated at high temperatures, limiting high-temperature performance improvement.

HP-A asphalt showed rutting factor decrease during initial short-term aging, which was temporary softening caused by rapid volatilization of light components. As aging deepened, oxidation products gradually accumulated, and rutting factor began to recover and exceed unaged levels.

3.4 Chemical functional group index aging behavior

3.4.1 Carbonyl aging index

Figure 7 illustrates the temperature-dependent rutting factor evolution of four modified asphalts across different aging stages (Li et al., 2021; Tan et al., 2020). Aging processes substantially alter asphalt rheological properties, with all samples exhibiting varying degrees of rutting factor enhancement, though through fundamentally different mechanisms. HP-C asphalt demonstrated pronounced rutting factor increases following short-term aging, rising from 45.3 kPa to 67.8 kPa at 64°C—representing a 49.7% enhancement. This improvement stems from oxidative formation of polar functional groups (carbonyls, sulfoxides) that strengthen intermolecular associations and enhance the material's elastic modulus (Zhang H. et al., 2018). After long-term aging, the rutting factor further increased to 78.2 kPa, though at a reduced rate (15.3%), suggesting that oxidative reactions approach thermodynamic equilibrium under prolonged exposure.

SBS asphalt exhibited distinctly different aging characteristics (Wang et al., 2021). Following short-term aging, significant rutting factor increases occurred in the low-temperature regime, while high-temperature performance improvements remained modest. This selective enhancement reflects the sequential

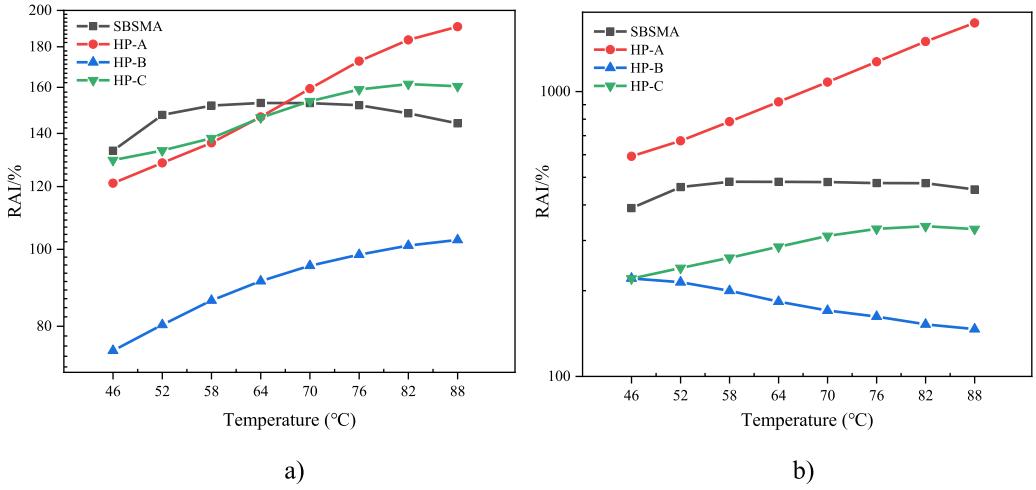

FIGURE 6
Rutting factor of different types of asphalt and their aging index RAI. **(a)** Short-term aging **(b)** Long-term aging.

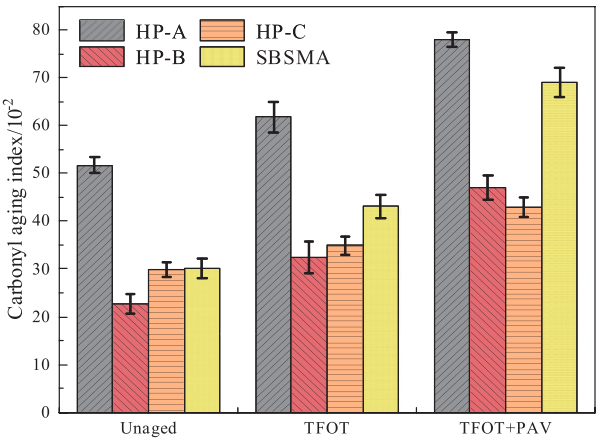

FIGURE 7
Carbonyl aging index of different asphalts.

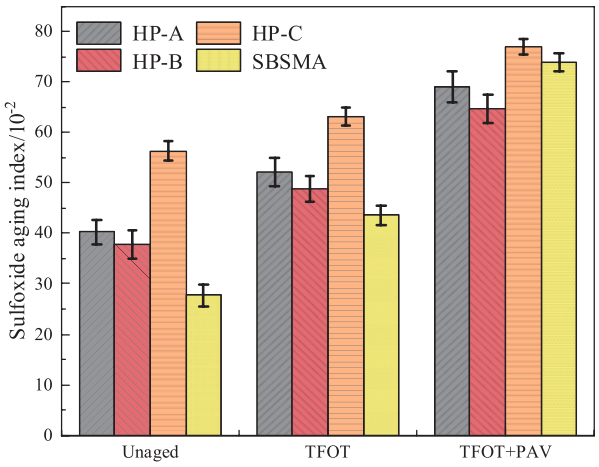

FIGURE 8
Sulfoxide aging index of different asphalts.

oxidation of SBS molecular architecture: preferential oxidation of butadiene segment double bonds initially generates crosslinking sites that enhance low-temperature elastic recovery, while thermal softening of styrene hard domains continues to dominate high-temperature response, limiting overall high-temperature performance gains.

HP-A asphalt displayed unique initial behavior, with rutting factors actually decreasing during early short-term aging—a phenomenon attributed to temporary softening caused by rapid volatilization of maltene fractions. As aging progressed, the accumulation of oxidative products (primarily asphaltenes formed from resin oxidation) gradually restored and eventually elevated rutting factors above unaged baseline levels. This biphasic response reflects the competing effects of volatile loss versus oxidative hardening that characterize HP-A asphalt's aging progression.

3.4.2 Sulfoxide aging index

The sulfoxide aging index results presented in Figure 8 provide critical insights into sulfur compound oxidation pathways within asphalt matrices. Sulfoxide groups (S=O) represent key intermediate products in the oxidative transformation of sulfur-containing compounds, with their concentration changes serving as reliable indicators of oxidative degradation in sulfur-bearing asphalt constituents (Duan et al., 2025). HP-B asphalt exhibited the most pronounced sulfoxide aging index increase at 29.28%, substantially exceeding other samples. This elevated oxidative susceptibility directly correlates with the inherently high sulfur content characteristic of BA-B crude oil source, providing abundant reactive substrates for oxidative transformation.

HP-A asphalt demonstrated a more moderate sulfoxide increase of 22.78%, consistent with its relatively lower sulfur content profile. SBS asphalt presented the most dramatic sulfoxide accumulation, reaching 57.41%, attributed to the oxidative degradation mechanisms specific to styrene-butadiene-styrene copolymers. The preferential oxidative cleavage of unsaturated

butadiene segments generates sulfur-containing radical species that accelerate sulfoxide formation, while the comparative thermal stability of styrene domains provides only partial mitigation of this oxidative cascade.

HP-C asphalt demonstrated superior oxidative stability with the minimal sulfoxide aging index increase of only 18.5%, further validating its exceptional anti-aging characteristics. The abundant phenolic and aromatic compounds inherent in BA-C asphalt function as effective radical scavengers, intercepting sulfur-derived free radicals generated during oxidative processes and effectively terminating propagating chain reactions. This natural antioxidant network provides comprehensive protection against sulfur compound oxidation, maintaining chemical stability throughout extended aging exposure.

4 Conclusion

In this paper, the compatibility between three different chemically toughened high-performance asphalt components and SBS-modified asphalt and the effect on the aging behavior were investigated. The main conclusions are as follows:

- HP-C asphalt demonstrates exceptional dual-high characteristics with a softening point of 78.2°C and Brookfield viscosity of 4.85 Pa·s, representing 17.8% and 32.4% improvements over SBS modified asphalt respectively. It exhibits the highest rutting factor, strongest shear deformation resistance, and optimal storage stability, making it ideal for high-temperature regions and heavy-duty traffic applications.
- HP-C asphalt shows superior long-term aging performance with the lowest softening point increment (4.2°C) and viscosity aging index (6.1%), while SBS modified asphalt exhibits poor long-term resistance with a viscosity aging index of 103.8%. The abundant aromatics in HP-C asphalt act as natural antioxidants, effectively retarding oxidation processes.
- Different asphalts exhibit distinct temperature responses during aging. HP-C asphalt shows increased rutting factor aging above 76°C, SBS modified asphalt demonstrates improved rheological properties above 70°C due to molecular network restructuring, while HP-A and HP-B maintain stable performance across high-temperature ranges.
- SBS modified and HP-B asphalts undergo oxidative crosslinking to form high molecular weight gel networks, while HP-A and HP-C asphalts primarily experience chain scission reactions. FTIR analysis confirms HP-B shows the highest sulfoxide aging index (29.3%) due to sulfur content, while HP-C demonstrates excellent antioxidant properties with low carbonyl (0.098) and sulfoxide (18.5%) aging indices.

5 Future research recommendation

Future research is recommend to focus on four key areas: analyzing the interaction mechanisms between key oil source components (aromatics, sulfur content) and modifiers to develop quantitative composition-structure-performance models; expanding validation across diverse climatic scenarios to assess system universality; conducting long-term field monitoring to verify laboratory-field aging correlations; and optimizing modifiers to enhance performance under extreme conditions and promote engineering applications.

Data availability statement

The original contributions presented in the study are included in the article/supplementary material, further inquiries can be directed to the corresponding author.

Author contributions

BH: Conceptualization, Project administration, Funding acquisition, Writing – original draft. CW: Writing – review and editing, Formal Analysis, Software, Methodology, Investigation, Visualization, Validation. YY: Writing – review and editing, Resources, Project administration. YW: Project administration, Funding acquisition, Writing – review and editing. YZ: Writing – review and editing, Visualization, Formal Analysis. RJ: Validation, Writing – review and editing, Visualization.

Funding

The author(s) declare that financial support was received for the research and/or publication of this article. This work was supported by the Transportation Science and Technology Program of Hunan Province (grant number 202509). The authors gratefully acknowledge their financial support.

Conflict of interest

Authors BH, YW were employed by Hunan Provincial Expressway Group Co., Ltd.

Author YY was employed by Modern Investment Co., Ltd.

The remaining authors declare that the research was conducted in the absence of any commercial or financial relationships that could be construed as a potential conflict of interest.

Generative AI statement

The author(s) declare that no Generative AI was used in the creation of this manuscript.

Publisher's note

References

Amini, N., and Hayati, P. (2020). Effects of CuO nanoparticles as phase change material on chemical, thermal and mechanical properties of asphalt binder and mixture. *Constr. Build. Mater.* 251, 118996. doi:10.1016/j.conbuildmat.2020.118996

Caputo, P., Porto, M., Angelico, R., Loise, V., Calandra, P., and Rossi, C. O. (2020). Bitumen and asphalt concrete modified by nanometer-sized particles: Basic concepts, the state of the art and future perspectives of the nanoscale approach. *Adv. Colloid Interface Sci.* 285, 102283. doi:10.1016/j.cis.2020.102283

Chen, S., Zhang, B., He, X., Su, Y., Liu, Q., and Xu, H. (2022). Research on mechanical-activated nanoscale bentonite and surface aging behavior of its modified asphalt. *Constr. Build. Mater.* 321, 126356. doi:10.1016/j.conbuildmat.2022.126356

Chen, Z., Zhang, H., Duan, H., Wu, C., and Zhang, S. (2021). Long-term photo oxidation aging investigation of temperature-regulating bitumen based on thermochromic principle. *Fuel* 286, 119403. doi:10.1016/j.fuel.2020.119403

Duan, H., Zhang, H., Lv, S., Lu, W., Ge, D., Jiang, R., et al. (2024). Insight into synergistic effect of zinc oxide/expanded vermiculite composite (ZnO/EVMT) on bituminous mixture performances under different aging conditions. *Constr. Build. Mater.* 446, 137945. doi:10.1016/j.conbuildmat.2024.137945

Duan, H., Zhang, H., Lv, S., Lu, W., Ge, D., Jiang, R., et al. (2025). Revealing aging behavior retarding mechanism of zinc oxide/expanded vermiculite composite modified bituminous mixture. *Constr. Build. Mater.* 468, 140388. doi:10.1016/j.conbuildmat.2025.140388

Duan, H., Zhu, C., Zhang, H., Zhang, S., Xiao, F., and Amirkhanian, S. (2023). Investigation on rheological characteristics of low-emissions crumb rubber modified asphalt. *Int. J. Pavement Eng.* 241 (1), 2164891. doi:10.1080/10298436.2023.2164891

Han, S., Dong, S., Liu, M., Han, X., and Liu, Y. (2019). Study on improvement of asphalt adhesion by hydrated lime based on surface free energy method. *Constr. Build. Mater.* 227, 116794. doi:10.1016/j.conbuildmat.2019.116794

Han, S., Dong, S., Yin, Y., Liu, M., and Liu, Y. (2020). Study on the effect of hydrated lime content and fineness on asphalt properties. *Constr. Build. Mater.* 244, 118379. doi:10.1016/j.conbuildmat.2020.118379

Hu, J., Wu, S., Liu, Q., Hernandez, M. I. G., Zeng, W., and Xie, W. (2017). Study of antiultraviolet bitumen modifiers and their antiageing effects. *Adv. Mater. Sci. Eng.* 2017, 9595239.

Lesueur, D., Petit, J., and Ritter, H. J. J. R. M. (2013). The mechanisms of hydrated lime modification of asphalt mixtures: a state-of-the-art review. *Road Mater. Pavement Des.* 14 (1), 1–16. doi:10.1080/14680629.2012.743669

Li, X., Zhou, Z., Ye, J., Wang, S., and Diab, A. (2021). High-temperature creep and low-temperature relaxation of recycled asphalt mixtures: evaluation and balanced mix design. *Constr. Build. Mater.* 310, 125222. doi:10.1016/j.conbuildmat.2021.125222

Li, Y., Dong, R., and Qin, Y. (2024). Characteristics of carbon black recycled from lightly pyrolyzed tire rubber and its impact on the high-temperature performance of asphalt. *Constr. Build. Mater.* 428, 136307. doi:10.1016/j.conbuildmat.2024.136307

Office, J. E., Chen, J., Dan, H., Ding, Y., Gao, Y., Guo, M., et al. (2021). New innovations in pavement materials and engineering: a review on pavement engineering research 2021. *J. Traffic Transp. Eng.* 8 (6), 815–999. doi:10.1016/j.jtte.2021.10.001

Tan, G., Wang, W., Cheng, Y., Wang, Y., and Zhu, Z. (2020). Master curve establishment and complex modulus evaluation of SBS-modified asphalt mixture reinforced with basalt fiber based on generalized sigmoidal model. *Polymers-Basel* 12 (7), 1586. doi:10.3390/polym12071586

Tan, Y., Zhang, L., and Xu, H. (2012). Evaluation of low-temperature performance of asphalt paving mixtures. *Cold Regions Sci. Technol.* 70, 107–112. doi:10.1016/j.coldregions.2011.08.006

Vestena, P. M., Schuster, S. L., de Almeida, J. , P. O. B., Faccin, C., Specht, L. P., and da Silva Pereiras, D. J. C. (2021). Dynamic modulus master curve construction of bituminous mixtures: error analysis in different models and field scenarios. *Constr. Build. Mater.* 301, 124343.

Wang, J., Zhang, H., and Zhu, C. (2020). Effect of multi-scale nanocomposites on performance of asphalt binder and mixture. *Constr. Build. Mater.* 243, 118307. doi:10.1016/j.conbuildmat.2020.118307

Wang, Q., Min, Z., Wong, Y. D., Li, M., and Huang, W. (2023). Evaluation of properties and aging resistance of epoxy asphalt composite modified by ultraviolet absorber. *J. Appl. Polym. Sci.* 140 (22), e53913. doi:10.1002/app.53913

Wang, R., Yue, M., Xiong, Y., and Yue, J. (2021). Experimental study on mechanism, aging, rheology and fatigue performance of carbon nanomaterial/SBS-modified asphalt binders. *Constr. Build. Mater.* 268, 121189. doi:10.1016/j.conbuildmat.2020.121189

Wang, T., Xiao, F., Amirkhanian, S., Huang, W., and Zheng, M. (2017). A review on low temperature performances of rubberized asphalt materials. *Constr. Build. Mater.* 145, 483–505. doi:10.1016/j.conbuildmat.2017.04.031

Xing, H., Liang, Y., Liu, G., Zhang, Y., Liu, X., and Fu, W. (2020). Organically treating montmorillonite with dual surfactants to modify bitumen. *Constr. Build. Mater.* 264, 120705. doi:10.1016/j.conbuildmat.2020.120705

Xu, S., Liu, L., Jia, X., Tighe, S., Zhang, C., Ma, H., et al. (2022). Investigation of aging resistance of organic layered double hydroxide/antioxidant composite-modified asphalt. *ACS Sustain. Chem. & Eng.* 11 (1), 267–277. doi:10.1021/acssuschemeng.2c05344

Zhang, D., Chen, Z., Zhang, H., and Wei, C. (2018). Rheological and anti-aging performance of SBS modified asphalt binders with different multi-dimensional nanomaterials. *Constr. Build. Mater.* 188, 409–416. doi:10.1016/j.conbuildmat.2018.08.136

Zhang, G., Qiu, J., Zhao, J., Wei, D., and Wang, H. (2020). Development of interfacial adhesive property by novel anti-stripping composite between acidic aggregate and asphalt. *Polymers-Basel* 12 (2), 473. doi:10.3390/polym12020473

Zhang, H., Chen, Z., Xu, G., and Shi, C. (2018). Evaluation of aging behaviors of asphalt binders through different rheological indices. *Fuel* 221, 78–88. doi:10.1016/j.fuel.2018.02.087

Zhang, H., Duan, H., Zhu, C., Chen, Z., and Luo, H. (2021). Mini-review on the application of nanomaterials in improving anti-aging properties of asphalt. *Energy & Fuels* 35 (14), 11017–11036. doi:10.1021/acs.energyfuels.1c01035

Zhang S., S., Hong, H., Zhang, H., and Chen, Z. (2021). Investigation of anti-aging mechanism of multi-dimensional nanomaterials modified asphalt by FTIR, NMR and GPC. *Constr. Build. Mater.* 305, 124809. doi:10.1016/j.conbuildmat.2021.124809

Zhao, K., and Wang, Y. (2022). Improvements on the use of GPC to measure large-size microstructures in aged asphalt binders. *Int. J. Pavement Eng.* 23 (7), 2309–2319. doi:10.1080/10298436.2020.1852561

Zhao, P., Gao, D., Ren, R., Han, K., Yang, Z., Meng, W., et al. (2021). Short-term aging performance evaluation of asphalt based on principal component and cluster analysis. *J. Test. Eval.* 49 (1), 590–602. doi:10.1520/jte20180781

Zhu, C., Zhang, H., Xu, G., and Wu, C. (2018). Investigation of the aging behaviors of multi-dimensional nanomaterials modified different bitumens by Fourier transform infrared spectroscopy. *Constr. Build. Mater.* 167, 536–542. doi:10.1016/j.conbuildmat.2018.02.056

Zhu, C., Zhang, H., and Zhang, Y. (2019). Influence of layered silicate types on physical, rheological and aging properties of SBS modified asphalt with multi-dimensional nanomaterials. *Constr. Build. Mater.* 228, 116735. doi:10.1016/j.conbuildmat.2019.116735